Biochimica et Biophysica Acta, 986 (1989) 341–345
Elsevier

BBAMEM 70636

BBA Report

Selforganization of a membrane in synaptic geometry

Peter Fromherz

Abteilung Biophysik der Universität Ulm, Ulm-Eselsberg (F.R.G.)

(Received 28 June 1989)

Key words: Membrane; Ion channel; Diffusion; Electrophoresis; Neuromuscular junction; Morphogenesis

The selforganization of mobile membrane proteins in a synaptic structure is computed. The model of dissipative condensation is used which takes into account the intermolecular interactions due to electrical channel currents and electrophoretic charges as they occur in a leaky membrane. An instability of the homogeneous fluid mosaic of charged channels is observed in the region of the synapse. Periodic accumulations of channels appear which are modulated by the attraction of protein from the perisynaptic membrane. The sensitivity of the process with respect to the geometrical constraints and to electrochemical parameters is discussed.

Usually cell membranes of nerve and muscle are described either on the basis of an electrical circuit of capacitances and resistances [1] or of a mosaic of protein molecules in a lipid bilayer [2]. In a previous paper it has been shown how these two basic aspects of membrane structure are coupled to each other through the electrical properties of membrane proteins as their ion conductance and their electrophoretic charge [3]. Far from electrochemical equilibrium a structural instability may occur in a fluid mosaic of charged channels such that spatio-temporal patterns of protein density and of membrane potential appear. Numerical solutions have been described for an isolated one-dimensional system as a closed cable [4,5].

In the present paper three novel aspects are touched: (i) Membrane patterns in two dimensions are considered. (ii) The instable region of the membrane is open, embedded in a large stable surround. (iii) The electrical resistance along the membrane is assigned to an extracellular cleft. The details of geometry and parameters are chosen to resemble a neuromuscular junction.

The system. The membrane of a 'muscle' cell forms a cylinder (radius 24 μm) (Fig. 1, left) within a cylinder of 'tissue' (radius 36 μm). A 'neuron' approaches the 'muscle' cell up to a distance of 0.05 μm. Length and width of this synapse are 90 μm and 15 μm, respectively. A finite piece of the system is modelled by a planar membrane of length l'' and width w'' as separated from an impermeable wall by an 'extracellular' medium of thickness d'' (Fig. 1, right and Table I). A rectangular protrusion of this wall of length l' and width w' forms a synaptic cleft of thickness d'. The 'intracellular' space beneath the membrane is unbound. The model system is closed at its edges with respect to flow of proteins and current. (With respect to symmetric patterns, as studied here, the constraint is equivalent to a torus topology.)

The muscle membrane contains a kind of 'active' protein molecules A as characterized by a channel conductance Λ_A, an electrophoretic charge q_A as exposed to the extracellular space and a diffusion coefficient D_A.

The average density of the protein molecules is $\bar{n}_A$. Their average conductance is $g_A = \Lambda_A \cdot \bar{n}_A$. The conductance of the background is g_B. The total average conductance is $g = g_A + g_B$ with an average fraction of A-conductance $\alpha_A = g_A/g$. The reversal potentials are

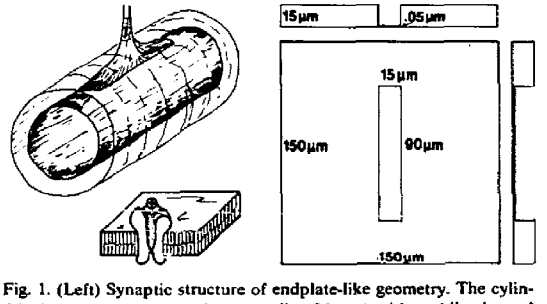

Fig. 1. (Left) Synaptic structure of endplate-like geometry. The cylindrical postsynaptical membrane (radius 24 μm) with mobile charged channel proteins (bottom) is enclosed in a passive cylinder of tissue (radius 36 μm). A neuronal contact forms a synapse (15 μm × 90 μm) which narrows the extracellular space down to 0.05 μm. (Right) Geometry of the planar model. The rounded dimensions of the system are indicated.

Correspondence: P. Fromherz, Abteilung Biophysik der Universität Ulm, D-7900 Ulm-Eselsberg, F.R.G.

E_A^0 and E_B^0. The average resting potential is $E_R = \alpha_A \cdot E_A^0 + (1-\alpha_A)\cdot E_B^0$.

The specific resistance of the extracellular medium is ρ. Surface resistances $r_S = \rho/d$ and electrotonic length constants $\lambda = (g \cdot r_S)^{-1/2}$ are defined for the synapse and the surround, respectively. The resistance of the intracellular space is neglected. The membrane has a specific capacitance c. The average electrical time constant is $\tau_V = c/g$.

Dynamics. The state of the postsynaptic membrane is described by the density $n_A(x,y,t)$ of open channel proteins and by the voltage (membrane potential) $v_M(x,y,t)$ of the extracellular medium (!) with respect to the intracellular spaces both as a function of the Cartesian coordinates x, y and the time t. A profile of potential across the extracellular medium is neglected ('plate-approximation'). The dynamics of the density $n_A(x,y,t)$ of charged channels is governed by Eqn. 1 which describes lateral diffusion and electrophoretic drift (conservation of molecules). The dynamics of the membrane potential $v_M(x,y,t)$ is governed by Eqn. 2 which expresses the balance of current densities across and along the membrane (conservation of charge). kT is the thermal energy. (The reversal potentials are defined for the extracellular space with respect to the intracellular space.) The actual parameters used for the evaluation of Eqns. 1 and 2 are given in Table I.

$$\frac{\partial n_A}{\partial t} = D_A \cdot \frac{\partial}{\partial x}\left[\frac{\partial n_A}{\partial x} + \frac{q_A}{kT}\cdot n_A \cdot \frac{\partial v_M}{\partial x}\right] + D_A \cdot \frac{\partial}{\partial y}\left[\frac{\partial n_A}{\partial y} + \frac{q_A}{kT}\cdot n_A \cdot \frac{\partial v_M}{\partial y}\right] \quad (1)$$

$$c \cdot \frac{\partial v_M}{\partial t} = \frac{\partial}{\partial x}\left[\frac{1}{r_S}\cdot\frac{\partial v_M}{\partial x}\right] + \frac{\partial}{\partial y}\left[\frac{1}{r_S}\cdot\frac{\partial v_M}{\partial y}\right] - g_B\cdot(v_M - E_B^0) - \Lambda_A \cdot n_A \cdot (v_M - E_A^0) \quad (2)$$

Numerical. For numerical integration of Eqn. 1 the normalized channel density $N_A = (n_A - \bar{n}_A)/\bar{n}_A$, and the normalized potential $V = (v_M - E_R)/(E_A^0 - E_B^0)$ are introduced. The normalized space coordinates are $X = x/1\ \mu m$ and $Y = y/1\ \mu m$. The normalized time is $T = t/\tau$ with the time constant of lateral transport $\tau = 1\ \mu m^2/D_A$. The dynamics $N_A(X,Y,T)$ is governed by Eqn. 3. The drive parameter is $\varepsilon_A = -q_A \cdot (E_A^0 - E_B^0)/kT$.

$$\frac{\partial N_A}{\partial T} = \frac{\partial}{\partial X}\left[\frac{\partial N_A}{\partial X} - \varepsilon_A\cdot(1+N_A)\cdot\frac{\partial V}{\partial X}\right] + \frac{\partial}{\partial Y}\left[\frac{\partial N_A}{\partial Y} - \varepsilon_A\cdot(1+N_A)\cdot\frac{\partial V}{\partial Y}\right] \quad (3)$$

This parabolic equation is solved by the finite difference method [6]. The membrane is partitioned into an equidistant grid of 101×101 elements of an area of 1.5

TABLE I

Parameters for synaptic selforganization

e_0, elementary charge. The potentials E_A^0, E_B^0 and E_R refer to the extracellular space with respect to intracellular space.

Geometry	Surround	Synapse
Length	$l'' = 151.5\ \mu m$	$l' = 91.5\ \mu m$
Width	$w'' = 151.5\ \mu m$	$w' = 16.5\ \mu m$
Thickness	$d'' = 15\ \mu m$	$d' = 50$ nm
Morphogenetic channel		
Conductance		$\Lambda_A = 30$ pS
Electrophoretic charge		$g_A = 5\ e_0$
Diffusion coefficient		$D_A = 0.1\ \mu m^2/s$
Circuit		
Channel density		$\bar{n}_A = 200\ \mu m^{-2}$
Conductance of channels		$g_A = 6$ nS/μm^2
Conductance of background		$g_B = 6$ nS/μm^2
Reversal potential of channels		$E_A^0 = -50$ mV
Reversal potential of background		$E_B^0 = 50$ mV
Resting potential		$E_R = 0$ mV
Specific resistance of medium		$\rho = 1\ M\Omega\cdot\mu m$
Surface resistance of synapse		$r_S'' = 20\ M\Omega$
Surface resistance of surround		$r_S' = 33\ k\Omega$
Electrotonic constant of synapse		$\lambda'' = 2\ \mu m$
Electrotonic constant of surround		$\lambda' = 35.3\ \mu m$
Capacitance		$c = 0.01$ pF/μm^2
Electrical time constant		$\tau_V = 0.83\ \mu s$

$\mu m \times 1.5\ \mu m$. (The synapse covers 11×61 elements.) The increment of normalized space of the grid is $\Delta = 1.5$. A explicit Euler-forward algorithm is used [4,7,8]. In case of a simple diffusion equation numerical instability would limit the time increment as $\Delta T < \Delta^2/4 = 0.563$. An increment of $\Delta T = 0.25$ is used here.

The dynamics of the normalized potential $V(X,Y,T^*)$ is governed by Eqn. 4. Time is normalized as $T^* = t/\tau_V$. The parameter $L = \lambda/1\ \mu m$ is the normalized length constant ($L = 2$ in the synapse, $L = 35.3$ in the perisynaptic space).

$$\frac{\partial V}{\partial T^*} = \frac{\partial}{\partial X}\left[L^2\cdot\frac{\partial V}{\partial x}\right] + \frac{\partial}{\partial Y}\left[L^2\cdot\frac{\partial V}{\partial y}\right] - V - \alpha_A\cdot(1-\alpha_A)\cdot N_A - \alpha_A\cdot N_A\cdot V \quad (4)$$

The potential follows the redistribution of channels almost instantaneously [3]. This electrical relaxation is evaluated by an explicit Euler-forward algorithm after each iteration step of channel dynamics. In a diffusion equation stability would limit the time increment as $\Delta T^* < \Delta^2/4 \cdot L^2 = 0.00045$ (surround). An increment of $\Delta T^* = 0.0002$ is used here.

Pattern formation is initiated by an increase of channel density by 20% in the central element of the array. 5184 time steps ΔT of channel dynamics are evaluated on a Cray-2 supercomputer corresponding to a real time of 216 min. Up to the 576th step 2500 time steps ΔT^* of electrical relaxation are inserted. Later only 500

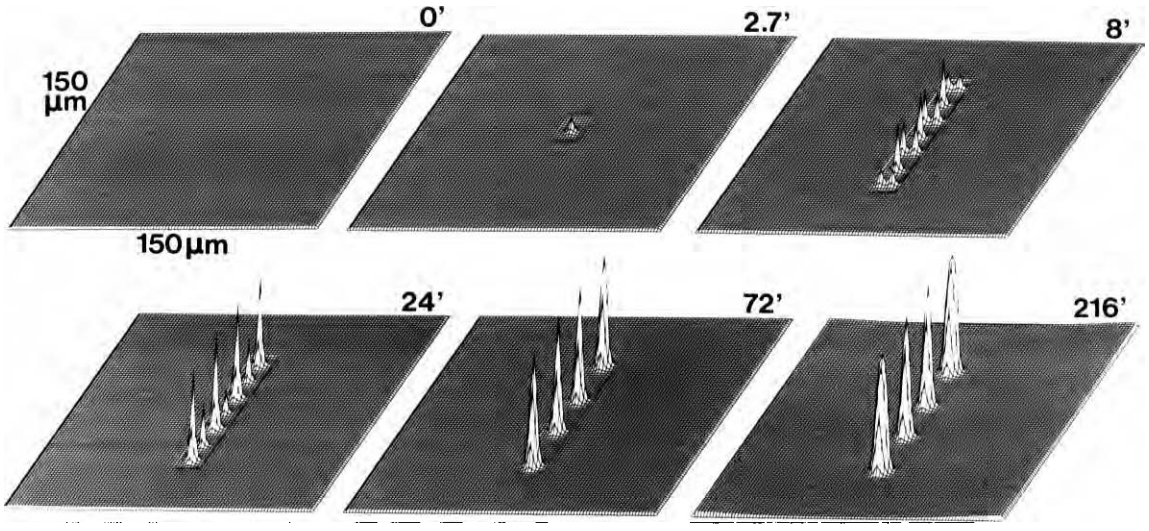

Fig. 2. Six stages of the development of channel density n_A in the postsynaptic membrane. The initial homogeneous density is 200 μm^{-2}. The time after a small perturbation in the center of the system is indicated. The electrochemical conditions of the system are discussed in the text.

relaxation steps are used. In test runs it has been checked that this truncation of relaxation does not cause significant deviations from true adiabatic dynamics.

Result. The pattern of channel density $n_A(x,y,t)$ is shown in Fig. 2 at six stages chosen at times $t = 0$, 2.66 min, 8 min, 24 min, 72 min and 216 min. The small symmetrical perturbation (Fig. 2: 0 min) initiates the development of a symmetrical pattern. (In a real membrane such perturbations occur intrinsically due to fluctuations.) A central accumulation of channels develops (Fig. 2: 2.7 min). Double peaks are formed as closest neighbours and other peaks further away along the synaptic zone (Fig. 2: 8 min). The double peaks fuse to simple accumulations such that a modulated periodic pattern is created with seven maximas at a distance of about 12 μm (Fig. 2: 24 min). The stronger peaks swallow the weak neighbours such that four peaks at a distance of about 25 μm are formed (Fig. 2: 72 min). Test runs show that the coalescence of the initial peaks in the synapse to a coarse pattern is induced by the coupling to the surround. At this stage the pattern spreads visibly into the perisynaptic space. Channels are attracted, the step of density is smeared out. The accumulations thicken and develop a plateau of a density round 5000 μm^{-2}. In the immediate surround a depletion of channels is induced. A slight accumulation appears at the periphery (Fig. 2: 216 min).

The computation reveals a scenario of selforganization of a postsynaptic membrane: (1) Structural instability of the fluid mosaic of charged channels within the synaptic cleft. (2) Growth of a periodic pattern within the synaptic cleft. (3) Coarsening of the initial pattern. (4) Formation of compact patches.

Discussion. To get some insight into the initiation of selforganization the result of numerical integration is compared with linear dynamics. In a previous paper it has been shown, for a one-dimensional system, that a close correlation exists between the quasi-stationary patterns and the linear growth constants [4].

A pattern in a rectangular membrane may be expressed by a superposition of plane waves as

$$N_A = \Sigma N_A^K \cdot \exp(iK_x x + iK_y y)$$

and

$$V = \Sigma V^K \cdot \exp(iK_x x + iK_y y)$$

Insertion into Eqns. 1 and 3 and Eqns. 2 and 4 leads to the linearized dynamics of the normalized amplitudes N_A^K and V^K of the waves of total wavenumber

$$K = \sqrt{K_x^2 + K_y^2}$$

In case of fast electrical relaxation the channel dynamics is described by rate equations [3]

$$dN_A^K/dt = k_K \cdot N_A^K$$

The growth constants k_K are defined by Eqn. 5. They are controlled by the pump parameter

$$P_A^0 = \varepsilon_A \cdot \alpha_A \cdot (1 - \alpha_A)$$

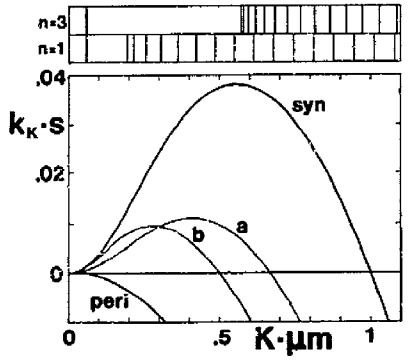

Fig. 3. (Bottom) Growth constant k_K versus total wavenumber K at a diffusion coefficient $D_A = 0.1\ \mu m^2/s$. The heavy lines refer to a pump parameter $P_A^0 = 5$. Syn, synaptic conditions with length constant $\lambda = 2\ \mu m$; peri, perisynaptic conditions with length constant $\lambda = 35.3\ \mu m$. The thin lines refer (a) to a reduced pump parameter $P_A^0 = 2.78$ at $\lambda = 2\ \mu m$ and (b) to an enhanced synaptic length constant $\lambda = 4\ \mu m$ at $P_A^0 = 5$. (Top) Spectra of the symmetric eigenmodes $n = 1, 3$ and $m = 1, 3, 5, 7, \ldots$ of the synapse. The heavy line at the left marks the lowest symmetrical mode ($m = n = 2$) of the perisynaptic membrane.

and by the length constant λ. They are scaled by the diffusion coefficient D_A.

$$k_K = D_A \cdot K^2 \cdot \left[\frac{P_A^0}{1 + (K \cdot \lambda)^2} - 1 \right] \tag{5}$$

Fig. 2 is computed with $D_A = 0.1\ \mu m^2/s$, $\alpha_A = 0.5$ and $\varepsilon_A = 20$ i.e. $P_A^0 = 5$. The spectra k_K are drawn in Fig. 3 for the synapse with $\lambda = 2\ \mu m$ and for the total membrane with $\lambda = 35.3\ \mu m$. For the total membrane the spectrum of growth constants crosses hardly the zero line. It is the formation of the synapse which gives rise to a wide spectrum of positive growth constants.

Only a discrete set of modes is allowed in the total membrane (vanishing flux at the edges) as $N_A^K \cdot \cos(K_x x) \cdot \cos(K_y y)$ with $K_x = m\pi/l''$ and $K_y = n\pi/w''$ $(m,n = 0,1,2,\ldots)$. With $l'' = w'' = 150\ \mu m$ even for the lowest symmetrical mode ($m = 2$, $n = 2$) the growth contant k_K is negative, as marked at the top of Fig. 3.

Also within the synapse only a discrete set of modes $N_A^K \cdot \sin(K_x x) \cdot \sin(K_y y)$ is allowed with $K_x = m\pi/l'$ and $K_y = n\pi/w'$ $(m,n = 1,3,3,\ldots)$ if the channel density at the edges is assumed to be fixed at $n_A = \bar{n}_A$ at the beginning with the normalized density fixed at $N_A = 0$. The m-spectra $m = 1, 3, 5, \ldots$ of the longitudinal symmetric modes are shown in Fig. 3 for two lateral modes $n = 1,3$. The modes $n = 1$, $m = 13$, 15, 17 and $n = 3$, $m = 1, 3, 5$ are favoured most.

Considering the discrete spectrum of the synapse and of the total membrane the rich dynamics during the development of synaptic structure (Fig. 2) must be attributed to a coupling of the two sets of instable eigenmodes $n = 1$ and $n = 3$ within the synapse and to a coupling of these modes to the stable modes of the surround. At early times the linear interference of the fastest modes determines the fundamental structure of the pattern. Nonlinear interactions lead to some adjustment. The coupling to the modes of the perisynaptic space becomes effective particularly at later times: Despite of their negative growth constant the lowest modes $(m,n = 0,2)$ are excited by the strong central depletion as induced by the synaptic accumulation. This coupling shapes the synaptic pattern without changing, however, its general appearance. The nature of the final pattern reflects the instability of the synaptic region.

The spectrum of rate constants is controlled solely by the pump parameter P_A^0 and by the length constant λ (Eqn. 5). For comparison a spectrum is shown in Fig. 3 for a weaker pump parameter $P_A^0 = 2.78$ and an enhanced length constant $\lambda = 4\ \mu m$. Only slow growth of long waves is allowed. The activation from $P_A^0 = 2.78$ to 5 at $\lambda = 2\ \mu m$ corresponds to an enhancement of channel density from $\bar{n} = 40\ \mu m^{-2}$ to $200\ \mu m^{-2}$. The activation from $\lambda = 4\ \mu m$ to $2\ \mu m$ at $P_A^0 = 5$ corresponds to a narrowing of the synaptic cleft from $d' = 0.2\ \mu m$ to $0.05\ \mu m$. Numerical integration of nonlinear dynamics confirms changes of the stationary pattern as indicated by the linear growth constants.

To emphasize selforganization the 'postsynaptic' membrane is assumed to be homogeneous at the beginning with respect to the leak conductivity and average density of the channels. A confinement of the open channel state to the synaptic region (closed channels in the surround) does not alter the dynamics significantly: The same local instability initiates the pattern. It attracts the charged proteins in the surround which contribute actively as they enter the synapse.

The geometry and the parameters used suggests a direct application of the model to the neuromuscular junction. There periodic aggregates of acetylcholine-receptor-channels (AChR) are obsered [9]. The feasibility of electrophoretic accumulation of AChR has been discussed [10,11]. Arguments against an activity of mobile channels have been a low mobility of most receptors and an obervation of aggregation even with most channels poisoned [12].

With respect to that issue five aspects may be pointed out resulting from the present study: (1) Aggregation of channels originates in an intrinsic instability of the membrane in the synaptic cleft. It is not initiated by gradients of potential at the edge of the synapse [10]. The primary pattern is amplified by accumulation of perisynaptical protein. (2) Dissipative condensation is based on an interaction of 'active' channels with passive leak conductivity of a different reversal potential. The presence of mobile charged channels (AChR) alone is

not sufficient. A direct electrical interaction with ion pumps is not involved [13]. (3) Synapse formation depends on at least two conductivities. One – due to the 'active' channels – is controlled by the presynaptic cell (growth, chemical gating), the other – the 'background' – may be controlled by the postsynaptic cell. (4) A saturation of channel density occurs in overcrowded regions – without taking into account short range molecular repulsion. The effect is due to a selfinduced reduction of channel current by the local depolarization of the membrane [4]. (5) A quantitative concept relates the geometrical, chemical and electrical parameters of a synapse to the nature of a pattern. On this basis a determination of the pertinent parameters in the real junction may decide whether primary selfassembly of AChR (before immobilization by the cell skeleton) is due to a dissipative condensation process or not.

Conclusions. Pattern formation in membranes by dissipative condensation relies on one hand on an appropriate density of mobile charged channel proteins and a supercritical activation of the membrane by ion gradients and on the other hand on a sufficiently short electrotonic length constant. The computation of the synaptic structure shows that a narrow extracellular space may provide well the required features of 'cable geometry'. Narrow extracellular spaces in tissues and narrow extraorganellar spaces within cells are quite common. Thus the approach may refer to a wide range of membrane-membrane junctions as e.g. to synapses between neurons, to neuron/glia-contacts, to growth cones, to the stacking of thylacoids in chloroplasts and of disks in rod outer segments and to the contact inner/outer membrane in mitochondria. Also artefacts in cell cultures as induced by the substrate may be considered. A particular study will be concerned with multiple synaptic junction – competing with each other – which may be of importance for learning and memory.

Generous support by the Fonds der Chemischen Industrie is acknowledged.

References

1 Hodgkin, A.L and Huxley, A.F. (1952) J. Physiol. (London) 117, 500–544.
2 Singer, S.L. and Nicolson, G.L. (1972) Science 175, 720–731.
3 Fromherz, P. (1988) Proc. Natl. Acad. Sci. USA 85, 6353–6357.
4 Fromherz, P. (1988) Ber. Bunsenges. Phys. Chem. 92, 1010–1016.
5 Fromherz, P. (1988) Biochim. Biophys. Acta 944, 108–111.
6 Richtmyer, R.D. (1957) Difference methods for initial value problems, Interscience, New York.
7 Ames, W.F. (1977) Numerical methods for partial differential equations, 2nd Edn. Academic Press, New York.
8 Gentzsch, W. (1984) Vectorization of computer programs with application to computational fluid dynamics, Vieweg, Braunschweig.
9 Schuetze, S.M. and Role, L.W. (1987) Annu. Rev. Neurosci. 10, 403–457.
10 Fraser, S.E. and Poo, M. (1982) Curr. Top. Develop. Biol. 17, 77–100.
11 McCloskey, M. and Poo, M. (1985) Int. Rev. Cytol. 87, 19–81.
12 Peng, H.B. and Poo, M. (1986) Trends Neurosci. 9, 125–129.
13 Jaffe, L.F. (1981) Phil. Trans. R. Soc. Lond. B. 295, 553–566.